Draft version August 18, 2026
Typeset using LaTeX **default** style in AASTeX7.0.1

A Radio-Bright Local Little Red Dot Analog

Luis F. Rodríguez[1], I. Félix Mirabel[2], Rosa A. González-Lópezlira[1] and Laurent Loinard[1]

[1] *Instituto de Radioastronomía y Astrofísica*
Universidad Nacional Autónoma de México, Apdo. Postal 3-72, Morelia, Michoacán 58089, Mexico
[2] *Instituto de Astronomía y Física del Espacio (IAFE)*
CONICET-Universidad de Buenos Aires, C1428 Buenos Aires, Argentina

ABSTRACT

The James Webb Space Telescope revealed the existence in the early Universe ($z > 4$) of large populations of little red dots (LRDs), compact red luminous sources that host rapidly growing supermassive black holes (SMBHs) surrounded by coeval nuclear starbursts. LRDs have defining properties, one of which is the absence of radio detections. LRDs could be radio-undetected because of their large distances. A way to investigate the radio properties of LRDs is to search for radio emission in their local analogs, the Local Little Red Dot (LLRD) galaxies at $z < 1$ with analogous properties to LRDs. We report the radio continuum detection of the LLRD analog J204837.26−002437.2 ($z =$ 0.4332, hereinafter J2048). This adds to the previous radio detection of two other LLRDs. However, with a flux density of 3.0±0.2 mJy at 3.0 GHz, J2048 is two orders of magnitude more radio luminous than the previous detections. The spectral index of α = -0.39±0.04 is consistent with moderately optically-thick synchrotron emission. The radio luminosity of J2048 is 1.2×10^{41} erg s^{-1}, in the lower end of the range defined by radio-loud giant elliptical galaxies and quasars of $L_R = 10^{41-46}$ erg s^{-1}. The expected radio luminosity of the SMBH associated with J2048 is estimated to be about an order of magnitude larger, suggesting that its radio luminosity could potentially be strongly dimmed. A cosmological ($z > 4$) LRD with radio luminosity similar to that of J2048 would be detectable using the VLA with moderately long integrations.

Keywords: Galaxy formation (595) — Massive stars (732) — Radio continuum emission (1340) — Supermassive black holes (1663)

1. INTRODUCTION

Several James Webb Space Telescope (JWST) surveys have discovered unexpected large populations of "Little Red Dots" (LRDs) at redshifts $z > 4$. These are extremely compact sources with average effective radius of less than a few hundred pc, widths of broad emission lines of up to 2000 km s^{-1}, and V-shaped spectral energy distributions (SEDs; e.g. J. Matthee et al. 2024; D. D. Kocevski et al. 2025; I. Labbe et al. 2025; H. B. Akins et al. 2025). LRDs reach a maximum density at $z \simeq 5$ and show an exponential decline in number at redshifts $z < 4$ (J.-B. Billand et al. 2026). This implies that local little red dot (LLRD) candidates are scarce.

The nature of the energy source that powers LRDs has been intensively debated since their discovery. As for quasars and ultra-luminous infrared galaxies (ULIRGs) in the past, the possible energy sources have been gravitational energy released by accreting supermassive (SMBHs) or intermediate mass black holes (IMBHs) and/or nuclear energy from exceptionally intense massive star formation. Several models have addressed this question through the analysis of the blue excess in the rest-frame ultraviolet (UV) SEDs of LRDs (K. Inayoshi 2025; K. Inayoshi & L. C. Ho 2025). These authors conclude that LRDs can be interpreted as a transient phase in early SMBH growth and that they may represent the long-sought missing link between SMBH seed formation and the emergence of luminous quasars.

If LRDs at cosmic dawn are indeed rapidly growing BHs, it is puzzling that they are not detected or are very dim in soft X-rays (< 10 keV) and that most of them have not been detected in radio wavelengths. The absence of X-rays has

Email: l.rodriguez@irya.unam.mx, mirabelfelix@gmail.com, r.gonzalez@irya.unam.mx, l.loinard@irya.unam.mx

been explained by cold gas absorption in BH atmospheres with densities $n_H \geq 10^9$ cm^{-3}, column densities $N_H \geq 10^{24}$ cm^{-2}, and turbulent velocities of ~500 km s^{-1} (R. Maiolino et al. 2025; X. Lin et al. 2026).

However, contrary to X-rays, radio emission from accreting BHs may not be totally or even partially absorbed by such column densities of cold neutral gas. In fact, radio jets from accreting stellar mass BHs are easily observed, even when the soft X-rays are completely obscured (L. F. Rodríguez & I. F. Mirabel 2025, and references therein). If radio emission could be detected in LRDs, it may be possible to discriminate from the morphology, time behavior and spectral index of the emission, between radio feedback from BHs and that from massive stars, i.e., between the energy generated by highly accreting IMBH/SMBHs, and that produced by multiple supernovae from rich clusters of massive stars. Besides, the detailed study of the radio emission may provide information to determine the specific phase in the evolution of the LRD studied, from its birth at cosmic dawn, believed to be dominated by feedback from a rapidly growing IMBH, to an intermediate (U)LIRG stage, to the possibly final post-LRD phase of a galaxy, which may end up with a dormant SMBH surrounded by an extended stellar component (J.-B. Billand et al. 2026).

LRDs, usually detected in the near-IR in the early universe, so far have been radio-undetected for unknown reasons, possibly influenced by their large distances and the limitations in our observational capabilities (e.g. G. Mazzolari et al. 2026; K. Perger et al. 2025; M. A. Latif et al. 2025). Several models have attempted to explain the absence of radio emission by invoking free-free absorption, synchrotron self-absorption, or the disruption of magnetic field coronae by super-Eddington accretion (G. Mazzolari et al. 2026; A. de Graaff et al. 2025).

Besides these models, a tentative cooling mechanism of radio BH-jets that to our knowledge has not yet been considered is Compton scattering, by UV photons from massive stars, of the highly relativistic electrons that produce the synchrotron emission of the BH-jets. For instance, in the case of BH-X-ray binaries (XRBs), where the donor star is very luminous, as for example in Cygnus X-1, this dimming mechanism of the radio jets is very important, of several orders of magnitude (I. F. Mirabel & L. F. Rodríguez 2022). This inverse Compton (IC) cooling by photons from massive stars affects the microscopic motions of the radiating ultra-relativistic electrons, suppressing the synchrotron radiation. This mechanism, however, does not affect the bulk motion of the ejecta. This is probably why LRDs and other types of active galactic nuclei (AGN) galaxies with nuclear starbursts may be capable of producing energetic mechanical feedbacks with radio "dark" jets. If BH-jets in LRDs and AGN in general co-exist with nuclear clusters of massive stars, the BH-jets may be radio weak but still produce massive outflows. Another radiation field that may produce inverse Compton weakening in the relativistic electrons of the jet is the cosmic microwave background, since its energy density scales as $(1+z)^4$ (G. Ghisellini et al. 2015).

Despite those dimming mechanisms, BH-jets may not be completely radio "dark". The black hole activity in the nuclei of galaxies may always be revealed by the presence of a compact radio-jet or an unresolved radio core (H. Falcke et al. 2004). Therefore, assuming that radio emission from LRDs at high redshifts may not have been detected because they reside at large distances and/or the observational capabilities are limited, we have initiated a search for radio emission from LLRDs with the U.S. National Radio Astronomy Observatory (NRAO) Very Large Array (VLA) and Very Long Baseline Array (VLBA), with the expectation that it might help understand why LRDs at high redshifts are radio-undetected, eventually leading to strategies (such as the determination of an optimal frequency), that could result in the radio detection of selected cosmological counterparts. An immediate way to test the different LRD models directly is by analyzing archived radio observations of LLRD candidates.

Using data from both the VLA archives and the Very Large Array Sky Survey (VLASS), radio emission was detected associated with two LLDRs: J1025+1402 and J1047+0739, at redshifts $z = 0.1-0.2$ (L. F. Rodriguez & I. F. Mirabel 2026). J1047+0739 is relatively nearby ($z = 0.1682$), radio faint, but clearly detected (117±8 μJy at 6.0 GHz). The radio emission associated with J1025+1402 ($z = 0.10067$) is fainter (45±10 μJy at 6.0 GHz) than that associated with J1047+0739. Furthermore, the radio emission is statistically significant but displaced by $\sim2''$ from the optical position. Two LRDs apparently in transition to QSOs, Forge I ($z = 2.871$) and Forge II (z= 2.930), have also been detected in the radio continuum (S. Fu et al. 2026). Finally, the AGN candidate PRIMER-COS 3866 at $z = 4.66$ was detected in the radio survey of A. J. Gloudemans et al. (2025).

Using a search method of optical-radio cross-matching we have seeked for radio emission in 48 LLRDs reported in the papers by X. Chen et al. (2026), W. Ding et al. (2026), R. Lin et al. (2025), X. Lin et al. (2026), K. Park et al. (2026), and J. Shangguan et al. (2026). A total of 14 of these sources were detected in the stacked VLASS images, for a success rate of 29%. Here, we report radio observations of the brightest of these sources: LLRD J204837.26-002437.2 (hereinafter J2048, as labeled by X. Chen et al. 2026), at $z = 0.4332$. It is a very interesting source, since it is comparatively very radio bright (3.1±0.1 mJy at 3.0 GHz, as we will see below), and an obvious target for VLBA follow-up observations. In Section 2, we present the properties of J2048, and in Section 3 the survey radio observations are described. We discuss how the radio parameters, in particular its radio luminosity, constrain the nature of J2048 in Section 4. The concept of supermassive stars, a possible explanation for the LRDs, and how they could be weak radio emitters is summarized in Section 5. Finally, a discussion of J2048 in the multiwavelength context is presented in Section 6 and our conclusions are outlined in Section 7.

2. THE GALAXY J2048

J2048 is one of the lowest-z analogs of LRDs, at $z = 0.4332$. It was identified by X. Chen et al. (2026), using new Gemini-North Multi-Object Spectrograph (GMOS) Integral Field Unit (IFU) spectroscopic observations, combined with archival multiband photometric SED data. The GMOS data reveal extended blue emission from a starburst with a star formation rate (SFR) of 400 $M_\odot$ yr^{-1}, with a high BH–to–stellar mass ratio of 60% and an extended, highly fast, ionized outflow. J2048 exhibits features similar to those of the high-z LRDs, such as a V-shaped SED in the UV and optical bands, as well as a compact, red continuum component that probably arises from a reddened AGN. It is located at intermediate redshifts ($0.1 < z < 1.0$) and was selected by X. Chen et al. (2020), from the cross-matched all-sky survey catalogs AKARI (far-IR) and Wide-field Infrared Survey Explorer (WISE; NIR and MIR), and the spectroscopic Sloan Digital Sky Survey (SDSS, optical) catalog. A compact red continuum and a broad Hα line from the AGN broad line region (BLR) were newly detected in the Gemini/GMOS observation of J2048.

The blue-excess is spatially extended and emitted from its intense starburst that is estimated has been taking place over the recent past (∼20 Myr). A compact red continuum in the NIR, and the BLR Hα line indicate an obscured AGN with $A_V = 6.3$, which corresponds to a bolometric luminosity of $10^{13.6}$ $L_\odot$. This high luminosity is consistent with J2048 being an ULIRG (D. B. Sanders & I. F. Mirabel 1996). J2048 also exhibits extended narrow line emission lines (X. Chen et al. 2026). It is believed that these extended narrow lines are ionized by stellar light of young stars with the BPT diagnostic, used to identify the dominant source of ionization in emission-line galaxies (J. A. Baldwin et al. 1981; L. J. Kewley et al. 2001). The corresponding instantaneous SFR estimated using the extinction-corrected fluxes of the narrow Hα or [O II] lines are 140 ± 10 or 100 ± 20 $M_\odot$ yr^{-1}, respectively, utilizing the empirical functions of D. Calzetti (2013) and R. C. Kennicutt et al. (2009). The SMBH of J2048 is extremely overmassive. X. Chen et al. (2026) estimate the BH mass from the AGN optical luminosity and the line width of the BLR Hα. Following the empirical relation of Y. Shen & X. Liu (2012) they derive $M_{BH} = 10^{10.2}$ $M_\odot$. They also obtain a stellar mass of $M_* = 10^{10.4}$ $M_\odot$, by fitting the photometric SED with a stellar population synthesis model. Then, X. Chen et al. (2026) derive a BH to stellar mass ratio, M_{BH}/M_*, of $\simeq$0.6, which is approximately two orders of magnitude larger than the ratio for local E/S0-type galaxies with a similar stellar mass M_* (A. E. Reines & M. Volonteri 2015).

J2048 possesses a fast ionized outflow, which is revealed by the blueshifted, broad wings in profiles of all emission lines in the integrated spectrum (X. Chen et al. 2026). The outflow wings dominate the line profiles of the [O III] 4959, 5007 Å doublet with a flux fraction of 84%. The [O III] outflow has two components, a primary wing, with V_s of -500 ± 20 km s^{-1} and FWHM of 1360 ± 30 km s^{-1} and a secondary wing with V_s of -2250 ± 30 km s^{-1} and FWHM of 1110 ± 60 km s^{-1}. The high [O III]/Hβ flux ratio implies that the fast outflowing gas is ionized by an AGN. The time-averaged mass-loss rate and kinetic power are estimated to be 160 $M_\odot$ yr^{-1} and $10^{44.3}$ erg s^{-1}, respectively.

3. RADIO SURVEYS

3.1. *NRAO Very Large Array Survey (VLASS)*

We have developed our program to search for radio continuum emission from local ($z < 1$) analogs of the LRDs as follows. A first step involves looking for relatively bright (> 0.5 mJy) sources in the NRAO Very Large Array Sky Survey (VLASS; M. Lacy et al. 2020; A. Kimball et al. 2026). This survey is being made in S-band (2−4 GHz, hereafter referred to as 3 GHz), covering the entire sky at Dec $> -40°$. Three epochs of observation have been completed and the fourth and last one is currently underway. To search for radio detections we did a visual inspection of the interactive Hierarchical Progressive Survey (HiPS) images, available at https://vlass-dl.nrao.edu/vlass/HiPS/MedianStack/Quicklook/. This data format allows users to quickly browse and zoom into very large astronomical images.

J2048 was clearly detected in all four epochs available, and the Flexible Image Transport System (FITS; D. C. Wells et al. 1981; W. D. Pence et al. 2010) individual images were analyzed to determine the total flux density of the associated radio source using the software package Astronomical Image Processing System (AIPS; E. W. Greisen 1990, 2003) of NRAO. In Table 1 we show the epoch, telescope, survey, central frequency, bandwidth and angular

Table 1. Surveys used in this paper

Epoch	Telescope	Survey	Central Frequency (GHz)	Bandwidth (GHz)	Angular Resolution	Total Flux Density (mJy)
1996-Sep-05	VLA	NVSS	1.40	0.1	$\simeq 45''$	4.0±1.1
2011-Mar-31	VLA	FIRST	1.40	0.05	$\simeq 5''$	3.6±0.3
2014-2024	LOFAR	LoTSS	0.144	0.048	$\simeq 9''$	9.7±0.9
2017-Dec-16	VLA	VLASS	3.00	2.0	$\simeq 3''$	3.0±0.3
2020-Aug-05	VLA	VLASS	3.00	2.0	$\simeq 3''$	3.0±0.4
2020-Oct-16	ASKAP	RACS-low	0.88	0.288	$\simeq 15''$	4.6±0.7
2021-Jan-17	ASKAP	RACS-mid	1.37	0.144	$\simeq 10''$	4.0±0.3
2022-Jan-10	ASKAP	RACS-high	1.67	0.288	$\simeq 7''$	3.7±0.3
2023-Jan-21	VLA	VLASS	3.00	2.0	$\simeq 3''$	3.2±0.3
2025-Sep-18	VLA	VLASS	3.00	2.0	$\simeq 3''$	3.1±0.3

Note—Each mosaic of LoTSS was built from multiple runs and no single epoch can be given per source.

resolution of the observations, as well as the flux density of the source. The lack of significant time variability over the 8-year period of the VLASS observations is consistent with that observed in other LLRDs at other bands of the electromagnetic spectrum (C. J. Burke et al. 2025). A final image, made by averaging the VLASS four epochs, is shown in Figure 1. This stacked VLASS image provides the best signal-to-noise ratio (SNR≃15) to determine the parameters of the source, which we list in Table 2. The quoted uncertainty on the radio position, $\Delta\theta_S$, is statistical and is approximately given by (J. J. Condon 1997):

$$\Delta\theta_{\rm S} \simeq \theta_{\rm B}/(2 \times {\rm SNR}), \tag{1}$$

where θ_B is the angular size of the synthesized beam, and SNR is the signal-to-noise ratio of the detection. A more realistic error can be obtained by adding in quadrature a systematic astrometric error of $0\farcs1$, appropriate for VLASS images (M. Lacy et al. 2020; Y. A. Gordon et al. 2021).

Table 2. Parameters of the source from the averaged VLASS image

Parameter	J2048
RA(J2000)	$20^h\ 48^m\ 37\fs245 \pm 0\fs002$
Dec(J2000)	$-00^\circ\ 24'\ 37\farcs32 \pm 0\farcs04$
Central Frequency (GHz)	3.0
Bandwidth (GHz)	2.0
Total Flux Density (mJy)	3.0±0.2
Angular Dimension ($''$)	≤ 0.8
Proper Size (kpc)	≤ 4.7
Brightness Temperature (K)	$\geq$900

The upper limit to the angular size of the source was estimated using (J. J. Condon 1997):

$$\theta_{\rm S} \leq \theta_{\rm B}/\sqrt{\rm SNR}, \tag{2}$$

where θ_S is the angular size of the source. Using the Javascript calculator from E. L. Wright (2006) and assuming a flat Planck ΛCDM cosmology with $H_0 = 67.4\,{\rm km\,s^{-1}\,Mpc^{-1}}$, $\Omega_{\rm m} = 0.315$, and $\Omega_\Lambda = 0.685$ (Planck Collaboration et al. 2020), we find that, for a source at $z = 0.4332$, the angular diameter distance is $D_A = 1202$ Mpc and the luminosity distance is $D_L = 2468$ Mpc. The proper size of the source is given by $l = D_A\theta_S$, which results in an upper limit to the proper size of the source of ≤ 4.7 kpc. This upper limit is not stringent, but it will be greatly improved with the future VLBA observations.

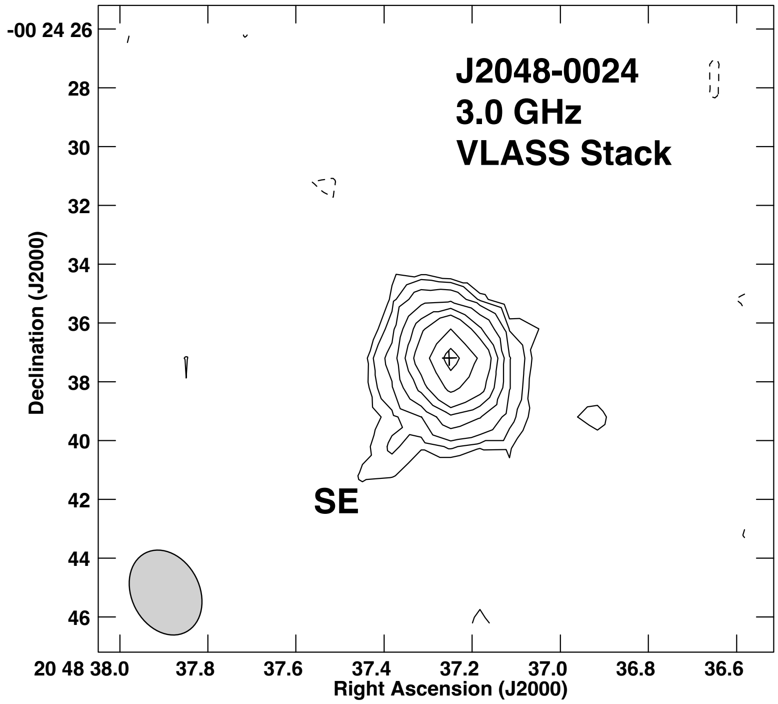

Figure 1. VLA contour 3.0 GHz image of the J2048-0024 region, made averaging the four epochs available from the Very Large Array Sky Survey (VLASS). Contours are -4, -3, 3, 4, 6, 10, 15, 20, 30, and 40 times 80.0 μJy beam^{-1}, i.e., the rms noise in this region of the image. The cross marks the optical position of the source from the Gaia Early Data Release 3 (Gaia Collaboration 2020). The morphology of the source consists of an unresolved component with a marginal protuberance about 4$''$ to the SE of the main component, which may be tracing a kpc jet or a second component in a merging ULIRG system. The tip of this protuberance is indicated with an SE label. The half-power full width of the beam ($2.''98 \times 2.''28$; $PA = +27.^\circ 2$) is shown in the bottom left corner.

The rest-frame brightness temperature of a source in Kelvin is given by (J. J. Condon & S. M. Ransom 2016):

$$T_b = 1.22 \times 10^3 (1+z) \left[\frac{S_\nu}{\mathrm{mJy}}\right] \left[\frac{\nu}{\mathrm{GHz}}\right]^{-2} \left[\frac{\theta_S}{''}\right]^{-2}, \tag{3}$$

which gives $T_b \geq 900$ K for J2048. As in the case of the proper size of the source, the lower limit to the rest-frame brightness temperature is not stringent, and higher angular resolution observations are required to improve it. These future observations can determine the rest-frame brightness temperature, a useful parameter to restrict the nature of the radio emission. A lower limit of about 10^6 K is needed to strongly favor a compact non-thermal AGN component (J. J. Condon 1992; L. K. Morabito et al. 2022).

3.2. *Other Surveys*

J2048 has been detected in several other surveys: the NRAO VLA Sky Survey Catalog (NVSS; J. J. Condon et al. 1998), the Faint Images of the Radio Sky at Twenty-cm (FIRST; R. H. Becker et al. 1995), the LOFAR Two-metre Sky Survey (LoTSS; T. W. Shimwell et al. 2026), and the Rapid Australian Square Kilometre Array Pathfinder Continuum Survey (RACS; D. McConnell et al. 2020). The parameters of these observations are given in Table 1. We have used these flux densities, as well as the one derived from the average image from all four VLASS observations, to determine α, the spectral index of the source, using the convention $S_\nu \propto \nu^\alpha$. In Figure 2, we show the flux densities as a function of frequency, and the least-squares fit to the data, given by

$$\log[\mathrm{S}_\nu(\mathrm{mJy})] = (0.65 \pm 0.02) - (0.39 \pm 0.04)\ \log[\nu(\mathrm{GHz})]. \tag{4}$$

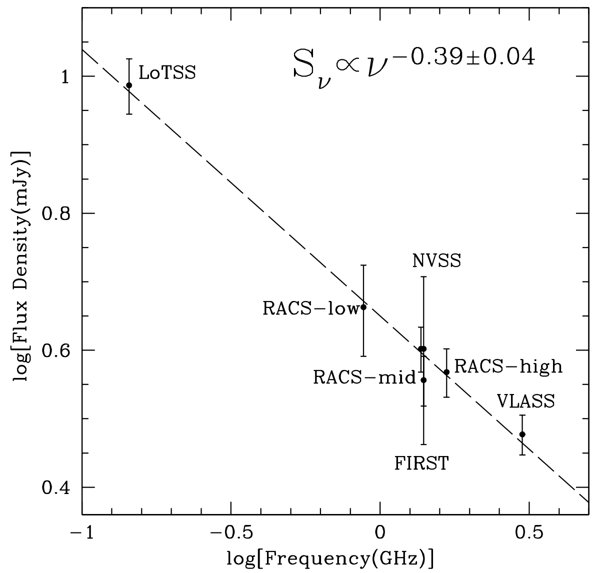

Figure 2. J2048 flux density as a function of frequency. The dashed line indicates the least-squares fit to the data, given in the text. The data points from the different surveys used are labeled. The spectral index of the fit is also given in the top of the figure.

The spectral index α = -0.39±0.04 is consistent with moderately optically-thick synchrotron emission, and rules out blackbody emission or dust emission, where spectral indices equal to or larger than 2 are expected. Its relative flatness suggests a potential blazar.

4. THE RADIO LUMINOSITY OF J2048

The radio luminosity L_R between the rest frequencies ν_2 and ν_1 of a cosmological source at a given z is calculated using the following equation:

$$L_{\rm R} = 4\pi\ D_{\rm L}^2\ S_\nu\ (1+z)^{-(\alpha+1)}\nu^{-\alpha}(\nu_2^{\alpha+1} - \nu_1^{\alpha+1})/(\alpha+1). \tag{5}$$

The radio luminosity has been estimated by assuming that the power-law spectrum, $S_\nu \propto \nu^\alpha$, is valid between 1 and 10 GHz. In this frequency range, spectral curvature is typically minimal (J. J. Condon 1992). For the parameters of J2048, we obtain $L_{\rm R} = 1.2 \times 10^{41}$ erg s^{-1}, two orders of magnitude larger than the radio luminosity of J1047+0739, the $z = 0.1682$ LLRD analog detected in the radio by L. F. Rodriguez & I. F. Mirabel (2026). The radio luminosity of J2048 places it in the lower end of the range defined by radio-loud giant elliptical galaxies and quasars, 10^{41-46} erg s^{-1} (A. K. Kembhavi & J. V. Narlikar 1999). Following K. I. Kellermann et al. (2016) we refer as radio-loud to those sources that exceed a monochromatic luminosity of $L_{\rm 5GHz} \simeq 10^{30.2}$ erg s^{-1} Hz^{-1} or a radio luminosity of $L_{\rm R} \simeq 10^{40}$ erg s^{-1}. Under these definitions, J2048 can be considered a radio-loud source.

We can use the measured flux density of J2048 to predict the flux density expected for an identical source located at cosmological distances. For a radio source with a power-law spectrum given by $S_\nu \propto \nu^\alpha$, the flux density measured at the same frequency and for two different z values is given by:

$$\left[\frac{S_\nu(z_1)}{S_\nu(z_0)}\right] = \left[\frac{1+z_0}{1+z_1}\right]^{-(\alpha+1)} \left[\frac{D_{\rm L}(z_0)}{D_{\rm L}(z_1)}\right]^2, \tag{6}$$

where z is the redshift, S_ν is the flux density, and D_L is the luminosity distance. In our case, the reference is J2048. The flux density for a source equal to J2048, located where the number density of LRDs peaks, i.e., z=5 (D_L = 47660 Mpc), is estimated by

$$S_\nu(z=5) = 7.0 \times 10^{-3}\ \ S_\nu(z=0.4332). \tag{7}$$

The expected flux density at 3.0 GHz is, then, $\simeq$20 μJy. This flux density can be detected with the VLA at the 10σ level with an on-source integration time of $\simeq$5 hours. With the next generation VLA (ngVLA; R. J. Selina et al. 2018) the on-source time required will be only about one minute. Realistically, taking into account slewing and calibration, a time in the tens of minutes will be required. For the reliable imaging of a resolved structure a proper *(u,v)* coverage is necessary, prolonging even further the required time. At the representative frequency of the Square Kilometer Array-low (SKA-low; R. Braun et al. 2020) of 200 MHz we expect a flux density of $\simeq$60 μJy. This flux density will be detected with the completed SKA-low at the 10σ level with an on-source integration time of $\simeq$40 minutes. Then, despite the higher flux density at lower frequencies, the better sensitivity of the ngVLA indicates this is the instrument of choice for future searches.

We note that the expected 3.0 GHz flux density for an identical source to J2048 located at z=5 of $\simeq$20 μJy is very similar to that measured for PRIMER-COS 3866 ($z = 4.66$) of 24.6 ± 4.2 μJy (V. Smolčić et al. 2017), suggesting that these sources are comparable in this respect. However, these sources have different spectral indices, -0.39 ± 0.04 for J2048 and -0.76 ± 0.10 for PRIMER-COS 3866 A. J. Gloudemans et al. (2025).

5. ABSENCE/SUPPRESSION OF X-RAY AND RADIO EMISSION IN LRD MODELS

Recently, models for the LRDs based on the concept of supermassive stars (SMSs) have been proposed (D. Nandal & A. Loeb 2026). These sources are posited to be metal-free gigantic stars powered by nuclear fusion. Their mass and radius can reach values of $\sim 10^6$ $M_\odot$ and $\sim 10^{14}$ cm, respectively, while their surface temperature is expected to be $\sim 1.5 \times 10^4$ K (D. Nandal & A. Loeb 2026). The monochromatic luminosity at a rest wavelength of 4050 Å is predicted to be $L_\lambda \sim 1.7 \times 10^{44}$ erg s^{-1} μm^{-1}, a value consistent with those measured in luminous LRDs, such as MoM-BH*-1 (R. P. Naidu et al. 2025) and The Cliff (A. de Graaff et al. 2025). No X-ray or radio emission is expected from an SMS. Indeed, the detection of X-ray emission from the LRD 3DHST-AEGIS-12014 (renamed as the "X-ray dot" or XRD), a compact source at $z = 3.28$ (R. E. Hviding et al. 2026), can be taken to weigh against the SMS hypothesis.

On the other hand, we have the black hole star (BH*, also called a quasi-star; R. P. Naidu et al. 2025; M. C. Begelman & J. Dexter 2026) model, which proposes an extraordinary object: an accreting supermassive black hole surrounded by a massive envelope of gas. In contrast to the SMSs, which derive their luminosity from nuclear fusion, the BH*s are heated by the energy released by the accreting disk of the central supermassive black hole. The existence of these remarkable objects was already speculated in papers written one to two decades ago (M. C. Begelman et al. 2006, 2008; W. H. Ball et al. 2011; T. Hosokawa et al. 2013). The model by A. D. Santarelli et al. (2026) proposes that a BH* has characteristic total mass, radius, temperature, luminosity and lifetime of $\sim 10^6$ M$_\odot$, $\sim 2.4 \times 10^5$ R$_\odot$, $\sim$5,000 K, $\sim 3.6 \times 10^{10}$ $L_\odot$ and $\sim$20 Myr, respectively. The BH* model strongly inhibits the X-ray and radio emissions, the first by the Compton opacity and the second by the free-free opacity. However, in the case of the radio emission (assumed to come from the jets from the central black hole), the jets can escape from the ionized envelope and become detectable in the radio. In the case of J2048 high angular resolution radio observations will help to establish if we are seeing the base of a relativistic jet or more extended lobes that could have escaped from the envelope of a BH*. These observations are in progress.

In the BH* model, the initial mass of the central black hole can be as small as $\sim$10 $M_\odot$, but it grows rapidly, in a scale of around 10^6 yr, reaching a million times the mass of the Sun at the end of its lifetime. The SMBH formed at the end of the life of the black-hole star could act as a massive seed for further growth and may help understand the existence of $\sim 10^9$ M$_\odot$ SMBHs early ($\sim$1 Gyr) in the universe.

6. THE RADIO OBSERVATIONS OF J2048 IN A MULTIWAVELENGTH CONTEXT

The radio source in J2048 has a spectral index of -0.39, which likely corresponds to a jet with partially optically thick radio emission. The main component has an angular diameter of less than 0.8 arcsec. At $z = 0.4332$, this upper limit to the angular diameter corresponds to an upper limit to the proper size of 4.7 kpc. In addition, the second, fainter component to the SE is displaced by $\simeq$3.6 arcsec from the center of the main component. This angular displacement corresponds to a physical distance in the plane of the sky of 21.0 kpc. From the comparison of the $\leq$4.7 kpc main component of the jet with Fig. 2 of X. Chen et al. (2026), it is inferred that such main component is embedded in and surrounded by a more extended region, of up to $r = 7$ kpc, of young stellar UV continuum, narrow Hα, and outflow [O III] line emissions. This suggests that the main component of the radio jet in J2048 could be constrained in length and luminosity by inverse Compton scattering of the UV photons by the highly relativistic electrons that would otherwise produce the synchrotron emission, a mechanism proposed in I. F. Mirabel & L. F. Rodríguez (2022) for BH-jets associated with high-mass star formation environments.

The radio flux density of 3-4 mJy at $z = 0.4332$ implies an intrinsic radio luminosity of 1.2×10^{41} erg s^{-1} between 1 and 10 GHz. What is the expected radio luminosity for a source like J2048?

From the fundamental-plane relation of A. Merloni et al. (2003) we have that

$$\log L_{5GHz} = 0.60 \log L_X + 0.78 \log\left(\frac{M_{\rm BH}}{M_\odot}\right) + 7.33, \tag{8}$$

where L_{5GHz} is the total radio luminosity derived from observations at 5 GHz and L_X is the 2–10 keV luminosity, both given in erg s^{-1}. $M_{\rm BH}$ is the mass of the black hole given in solar masses. A. Merloni et al. (2003) note that $\log(L_{5GHz})$ has a substantial scatter of $\sigma_{5GHz} = 0.88$.

The X-ray bolometric correction, κ_X is defined as

$$\kappa_X \equiv \frac{L_{\rm bol}}{L_X}, \tag{9}$$

where $L_{\rm bol}$ is the bolometric luminosity of the source. If the black hole is radiating at the Eddington luminosity, we can assume that

$$L_{\rm bol} = L_{\rm Edd} = 1.26 \times 10^{38} \left(\frac{M_{\rm BH}}{M_\odot}\right) {\rm erg\,s^{-1}}. \tag{10}$$

Therefore,

$$L_X = \frac{1.26 \times 10^{38}}{\kappa_X} \left(\frac{M_{\rm BH}}{M_\odot}\right) {\rm erg\,s^{-1}}. \tag{11}$$

Substituting this expression into the fundamental-plane relation gives

$$\log L_{5GHz} = 30.19 + 1.38 \log\left(\frac{M_{\rm BH}}{M_\odot}\right) - 0.60 \log(\kappa_X). \tag{12}$$

J2048 has $L_{\rm bol} = 10^{13.6\ L_\odot}$, which following F. Duras et al. (2020) implies $\kappa_X \simeq 80$. Finally, since $M_{\rm BH} = 10^{10.2}\ M_\odot$, we obtain $L_{5GHz} \simeq 10^{43.1\pm0.9}\ erg\ s^{-1}$ We note, however, that X. Chen et al. (2026) report an Eddington ratio of 0.08±0.01 for J2048, so the expected value will be $L_{5GHz} \simeq 10^{42.0\pm0.9}\ erg\ s^{-1}$. This radio luminosity is about one order of magnitude larger than that measured, suggesting that a suppression mechanism could be present. However, the scatter in the A. Merloni et al. (2003) relation is also about an order of magnitude, so the smaller radio luminosity could be simply due to the source being intrinsically weaker.

The suppressed radio emission of the jets, if present, should be expected to produce an inefficient radio emitting massive outflow. In fact, J2048 hosts a massive ionized outflow with extension of up to 3 kpc, a velocity of 2070± 40 km s^{-1}, a time-averaged mass-loss rate of 160 $M_\odot$ yr^{-1}, an outflow timescale of 0.7 Myr, and a kinetic power of $10^{44.3}$ erg s^{-1} (X. Chen et al. 2026). These authors propose that this outflow must be driven by AGN activity because of its high velocity, kinetic power, and AGN-type ionization. They also found that the massive ionized outflow in J2048 is only marginally resolved, and unfortunately no preferred position angle was reported to compare with the radio morphology.

There are many evidences that, in LRD analogs, the concurrency of nuclear starbursts with an SMBH fed by dense cold gas could be common (e.g. P. G. Pérez-González et al. 2024; P. Rinaldi et al. 2025; I. Delvecchio et al. 2025; K. Inayoshi et al. 2026; Euclid Collaboration et al. 2026). J2048 is an ULIRG with an infrared luminosity (1–1000 μm) higher than 10^{12} $L_\odot$. In the local universe, there are advanced mergers of massive cold gas-rich galaxies with their respective nuclei closer than 10 kpc (D. B. Sanders & I. F. Mirabel 1996). D. B. Sanders et al. (1988) proposed that ULIRGs are the initial dust-enshrouded stage of quasars. They have high accretion rates of cold gas that feed both a nuclear SMBH and a starburst, as believed to be the case of LRDs in the early universe (K. Inayoshi et al. 2026). This is why the ULIRG J2048 qualitatively reflects the properties of high-z LRDs: it has a V-shaped SED, a blue continuum at rest UV wavelengths, a red continuum at rest optical wavelengths, and a large $M_{\rm BH}/M_*$ ratio of 60%. It is an analog of high-z LRDs in a late stage of evolution, when the merging process induces a nuclear starburst of 400 ± 60 $M_\odot$ yr^{-1}, and an X-ray-obscured AGN with a bright radio jet.

Close to the SMBH the LRDs will go radio-undetected because of the extremely large free-free opacity of the BH ionized envelope. From the parameters of the model of A. D. Santarelli et al. (2026) presented in Section 5 we estimate a characteristic electron density of $n_e \simeq 6.0 \times 10^{13}$ cm^{-3} and an emission measure of EM $\simeq 2.0 \times 10^{25}$ pc cm^{-6}. From the expression for free-free opacity (T. L. Wilson et al. 2022):

$$\tau_{\rm ff} \simeq 3.28 \times 10^{-7} \left(\frac{T_e}{10^4\,{\rm K}}\right)^{-1.35} \left(\frac{\nu}{\rm GHz}\right)^{-2.1} \left(\frac{\rm EM}{\rm pc\ \ cm^{-6}}\right), \tag{13}$$

we obtain an enormous opacity, $\tau_{\rm ff} \simeq 1.7 \times 10^{18}$ at 3.0 GHz. Radio emission from the central regions will not escape the envelope.

Outside of this envelope the jets may be silenced at radio due to the inverse Compton scattering by photons from the ionized envelope on the jet highly relativistic electrons that otherwise would produce the synchrotron emission. To explore this possibility we note that the energy losses of the relativistic electrons to synchrotron emission and IC scattering are proportional to the energy densities of the magnetic and radiation fields, respectively. From A. P. Lobanov (1998) and S. P. O'Sullivan & D. C. Gabuzda (2009) we find that at the surface of the envelope, at a distance of 0.005 pc from the AGN, a magnetic field of order 10^2 G is expected. The magnetic energy density at this location is then $\rm u_B = B^2/(8\ \pi) \simeq 4.0 \times 10^2$ erg cm^{-3}. For a spherical surface with radius R emitting a luminosity L, the radiation energy density will be given by $\rm u_{rad} = L/(4\pi R^2 c)$, where c is the speed of light. For $\rm L \simeq 3.6 \times 10^{10}\ L_\odot = 1.4 \times 10^{44}$ erg s^{-1}, and $\rm R \simeq 1.7 \times 10^{16}$ cm we obtain $\rm u_{rad} \simeq 1.3$ erg cm^{-3}. Since $\rm u_B/u_{rad} \simeq 300$ we conclude that IC cooling is unimportant in comparison to synchrotron cooling and will not significantly suppress the synchrotron emission.

7. CONCLUSIONS

Our conclusions can be summarized as follows.

1) The radio emission of J2048 at 3.0 GHz lacks significant time variability over an 8-year period of observations. This is consistent with the lack of significant time variability in observations of other LLRDs at different bands of the electromagnetic spectrum (C. J. Burke et al. 2025). The spectral index α = -0.39±0.04 of the radio emission is consistent with moderately optically-thick synchrotron emission, and rules out blackbody emission or dust emission. The spectrum flatness could indicate a potential blazar.

2) The upper limit to the diameter of the main radio component of the source is ≤4.7 kpc. The properties of this main radio component will be studied in detail by already proposed VLBA observations. The radio source in J2048 has a second component to the SE of the main component, with a total physical separation in the plane of the sky of 21.0 kpc. This second component could be the tip of an SMBH-jet escaping to the intergalactic medium, from the nuclear high densities of gas and radiation.

3) The radio luminosity of J2048 of 1.2×10^{41} erg s^{-1} place it in the lower end of the range defined by radio-loud giant elliptical galaxies and quasars of 10^{41-46} erg s^{-1} (A. K. Kembhavi & J. V. Narlikar 1999). The flux density at 3.0 GHz of a source like J2048 at z=5 is ≃20 μJy. This flux density can be detected with the VLA at the 10σ level with an on-source integration time of ≃5 hours. The ngVLA will achieve such a detection in a matter of minutes.

4) The radio luminosity of the SMBH of $10^{10.2}$ M$_\odot$ in J2048 (X. Chen et al. 2026) is expected to be about an order of magnitude larger than measured, suggesting that its radio luminosity could potentially be strongly dimmed. The suppressed energy of the relativistic electrons in the jets could convert them into an inefficient radio-synchrotron emitting massive outflow. In fact, J2048 hosts a massive ionized outflow with extension of up to 3 kpc with a kinetic power of $10^{44.3}$ erg s^{-1} (X. Chen et al. 2026).

5) J2048 appears to be an ULIRG with an infrared luminosity (1–1000 µm) of at least 10^{12} L$_\odot$. J2048 and ULIRGs in general may reflect the properties of cosmological LRDs because in both types of galaxies dense cold gas feeds at high rates nuclear starbursts and the growing of SMBHs.

ACKNOWLEDGMENTS

We thank an anonymous referee for valuable suggestions that improved the paper. This research has made use of the SIMBAD database, operated at CDS, Strasbourg, France. LFR thanks the financial support from grant CBF-2025-I-2471 of SECIHTI, México. RAGL acknowledges the financial support of DGAPA, UNAM, project IN106124. LL acknowledges the support of DGAPA-PAPIIT grant IN108324 and SECIHTI grant CBF-2025-I-109.

Facilities: NRAO VLA, CSIRO ASKAP

Software: astropy (Astropy Collaboration et al. 2013, 2018, 2022).

REFERENCES

Akins, H. B., Casey, C. M., Lambrides, E., et al. 2025, ApJ, 991, 37, doi: 10.3847/1538-4357/ade984

Astropy Collaboration, Robitaille, T. P., Tollerud, E. J., et al. 2013, A&A, 558, A33, doi: 10.1051/0004-6361/201322068

Astropy Collaboration, Price-Whelan, A. M., Sipőcz, B. M., et al. 2018, AJ, 156, 123, doi: 10.3847/1538-3881/aabc4f

Astropy Collaboration, Price-Whelan, A. M., Lim, P. L., et al. 2022, ApJ, 935, 167, doi: 10.3847/1538-4357/ac7c74

Baldwin, J. A., Phillips, M. M., & Terlevich, R. 1981, PASP, 93, 5, doi: 10.1086/130766

Ball, W. H., Tout, C. A., Żytkow, A. N., & Eldridge, J. J. 2011, MNRAS, 414, 2751, doi: 10.1111/j.1365-2966.2011.18591.x

Becker, R. H., White, R. L., & Helfand, D. J. 1995, Astrophysical Journal, 450, 559, doi: 10.1086/176166

Begelman, M. C., & Dexter, J. 2026, ApJ, 996, 48, doi: 10.3847/1538-4357/ae274a

Begelman, M. C., Rossi, E. M., & Armitage, P. J. 2008, MNRAS, 387, 1649, doi: 10.1111/j.1365-2966.2008.13344.x

Begelman, M. C., Volonteri, M., & Rees, M. J. 2006, MNRAS, 370, 289, doi: 10.1111/j.1365-2966.2006.10467.x

Billand, J.-B., Elbaz, D., Gentile, F., et al. 2026, A&A, 706, A29, doi: 10.1051/0004-6361/202556303

Braun, R., Bonaldi, A., Bourke, T., Keane, E., & Wagg, J. 2020, arXiv e-prints. https://arxiv.org/abs/1912.12699

Burke, C. J., Stone, Z., Shen, Y., & Jiang, Y.-F. 2025, arXiv e-prints, arXiv:2511.16082, doi: 10.48550/arXiv.2511.16082

Calzetti, D. 2013, in Secular Evolution of Galaxies, ed. J. Falcón-Barroso & J. H. Knapen, 419, doi: 10.48550/arXiv.1208.2997

Chen, X., Akiyama, M., Ichikawa, K., et al. 2020, ApJ, 900, 51, doi: 10.3847/1538-4357/aba599

Chen, X., Ichikawa, K., Akiyama, M., et al. 2026, ApJ, 999, 30, doi: 10.3847/1538-4357/ae3683

Condon, J. J. 1992, Annual Review of Astronomy and Astrophysics, 30, 575, doi: 10.1146/annurev.aa.30.090192.003043

Condon, J. J. 1992, ARA&A, 30, 575, doi: 10.1146/annurev.aa.30.090192.003043

Condon, J. J. 1997, PASP, 109, 166, doi: 10.1086/133871

Condon, J. J., Cotton, W. D., Greisen, E. W., et al. 1998, Astronomical Journal, 115, 1693, doi: 10.1086/300337

Condon, J. J., & Ransom, S. M. 2016, Essential Radio Astronomy

de Graaff, A., Rix, H.-W., Naidu, R. P., et al. 2025, A&A, 701, A168, doi: 10.1051/0004-6361/202554681

Delvecchio, I., Daddi, E., Magnelli, B., et al. 2025, A&A, 704, A313, doi: 10.1051/0004-6361/202557164

Ding, W., Kong, X., Guo, W.-J., et al. 2026, A&A, 709, L11, doi: 10.1051/0004-6361/202557889

Duras, F., Bongiorno, A., Ricci, F., et al. 2020, A&A, 636, A73, doi: 10.1051/0004-6361/201936817

Euclid Collaboration, Tumborang, A. A., Caputi, K. I., et al. 2026, arXiv e-prints, arXiv:2604.16178. https://arxiv.org/abs/2604.16178

Falcke, H., Körding, E., & Markoff, S. 2004, A&A, 414, 895, doi: 10.1051/0004-6361:20031683

Fu, S., Zhang, Z., Jiang, D., et al. 2026, Nature Astronomy, doi: 10.1038/s41550-026-02885-8

Gaia Collaboration. 2020, VizieR Online Data Catalog: Gaia EDR3 (Gaia Collaboration, 2020),, VizieR On-line Data Catalog: I/350. Originally published in: 2021A&A...649A...1G doi: 10.26093/cds/vizier.1350

Ghisellini, G., Haardt, F., Ciardi, B., et al. 2015, MNRAS, 452, 3457, doi: 10.1093/mnras/stv1541

Gloudemans, A. J., Duncan, K. J., Eilers, A.-C., et al. 2025, ApJ, 986, 130, doi: 10.3847/1538-4357/adddb9

Gordon, Y. A., Boyce, M. M., O'Dea, C. P., et al. 2021, ApJS, 255, 30, doi: 10.3847/1538-4365/ac05c0

Greisen, E. W. 1990, in Acquisition, Processing and Archiving of Astronomical Images, ed. G. Longo, G. Sedmak, & A. Ficarra (Napoli: Osservatorio Astronomico di Capodimonte), 125–142

Greisen, E. W. 2003, in Astrophysics and Space Science Library, Vol. 285, Information Handling in Astronomy – Historical Vistas, ed. A. Heck (Dordrecht: Kluwer Academic Publishers), 109–125, doi: 10.1007/0-306-48080-8_7

Hosokawa, T., Yorke, H. W., Inayoshi, K., Omukai, K., & Yoshida, N. 2013, ApJ, 778, 178, doi: 10.1088/0004-637X/778/2/178

Hviding, R. E., de Graaff, A., Liu, H., et al. 2026, ApJL, 1000, L18, doi: 10.3847/2041-8213/ae4c88

Inayoshi, K. 2025, ApJL, 988, L22, doi: 10.3847/2041-8213/adea66

Inayoshi, K., & Ho, L. C. 2025, arXiv e-prints, arXiv:2512.03130, doi: 10.48550/arXiv.2512.03130

Inayoshi, K., Murase, K., & Kashiyama, K. 2026, ApJ, 1000, 90, doi: 10.3847/1538-4357/ae42ce
Kellermann, K. I., Condon, J. J., Kimball, A. E., Perley, R. A., & Ivezić, Ž. 2016, ApJ, 831, 168, doi: 10.3847/0004-637X/831/2/168
Kembhavi, A. K., & Narlikar, J. V. 1999, Quasars and active galactic nuclei : an introduction
Kennicutt, Jr., R. C., Hao, C.-N., Calzetti, D., et al. 2009, ApJ, 703, 1672, doi: 10.1088/0004-637X/703/2/1672
Kewley, L. J., Dopita, M. A., Sutherland, R. S., Heisler, C. A., & Trevena, J. 2001, ApJ, 556, 121, doi: 10.1086/321545
Kimball, A., Lacy, M., Ott, J., et al. 2026, arXiv e-prints. https://arxiv.org/abs/2606.27414
Kocevski, D. D., Finkelstein, S. L., Barro, G., et al. 2025, ApJ, 986, 126, doi: 10.3847/1538-4357/adbc7d
Labbe, I., Greene, J. E., Bezanson, R., et al. 2025, ApJ, 978, 92, doi: 10.3847/1538-4357/ad3551
Lacy, M., Baum, S. A., Chandler, C. J., et al. 2020, PASP, 132, 035001, doi: 10.1088/1538-3873/ab63eb
Latif, M. A., Aftab, A., Whalen, D. J., & Mezcua, M. 2025, A&A, 694, L14, doi: 10.1051/0004-6361/202453194
Lin, R., Zheng, Z.-Y., Jiang, C., et al. 2025, ApJL, 980, L34, doi: 10.3847/2041-8213/adaaf1
Lin, X., Fan, X., Cai, Z., et al. 2026, ApJ, 997, 364, doi: 10.3847/1538-4357/ae2bdf
Lobanov, A. P. 1998, Astronomy and Astrophysics, 330, 79
Maiolino, R., Risaliti, G., Signorini, M., et al. 2025, MNRAS, 538, 1921, doi: 10.1093/mnras/staf359
Matthee, J., Naidu, R. P., Brammer, G., et al. 2024, ApJ, 963, 129, doi: 10.3847/1538-4357/ad2345
Mazzolari, G., Gilli, R., Maiolino, R., et al. 2026, A&A, 706, A372, doi: 10.1051/0004-6361/202453317
McConnell, D., Hale, C. L., Lenc, E., & et al. 2020, Publications of the Astronomical Society of Australia, 37, e048, doi: 10.1017/pasa.2020.41
Merloni, A., Heinz, S., & di Matteo, T. 2003, MNRAS, 345, 1057, doi: 10.1046/j.1365-2966.2003.07017.x
Mirabel, I. F., & Rodríguez, L. F. 2022, NewAR, 94, 101642, doi: 10.1016/j.newar.2022.101642
Morabito, L. K., Sweijen, F., Radcliffe, J. F., et al. 2022, Monthly Notices of the Royal Astronomical Society, 515, 5758, doi: 10.1093/mnras/stac2129
Naidu, R. P., Matthee, J., Katz, H., et al. 2025, arXiv e-prints, arXiv:2503.16596, doi: 10.48550/arXiv.2503.16596
Nandal, D., & Loeb, A. 2026, ApJ, 998, 124, doi: 10.3847/1538-4357/ae32f3
O'Sullivan, S. P., & Gabuzda, D. C. 2009, Monthly Notices of the Royal Astronomical Society, 400, 26, doi: 10.1111/j.1365-2966.2009.15428.x
Park, K., Torralba, A., Matthee, J., et al. 2026, arXiv e-prints, arXiv:2605.14233, doi: 10.48550/arXiv.2605.14233
Pence, W. D., Chiappetti, L., Page, C. G., Shaw, R. A., & Stobie, E. 2010, Astronomy & Astrophysics, 524, A42, doi: 10.1051/0004-6361/201015362
Pérez-González, P. G., Barro, G., Rieke, G. H., et al. 2024, ApJ, 968, 4, doi: 10.3847/1538-4357/ad38bb
Perger, K., Fogasy, J., Frey, S., & Gabányi, K. É. 2025, A&A, 693, L2, doi: 10.1051/0004-6361/202452422
Planck Collaboration, Aghanim, N., Akrami, Y., et al. 2020, A&A, 641, A6, doi: 10.1051/0004-6361/201833910
Reines, A. E., & Volonteri, M. 2015, ApJ, 813, 82, doi: 10.1088/0004-637X/813/2/82
Rinaldi, P., Bonaventura, N., Rieke, G. H., et al. 2025, ApJ, 992, 71, doi: 10.3847/1538-4357/adfa10
Rodríguez, L. F., & Mirabel, I. F. 2025, ApJ, 986, 108, doi: 10.3847/1538-4357/adda33
Rodriguez, L. F., & Mirabel, I. F. 2026, A&A, 707, L17, doi: 10.1051/0004-6361/202558326
Sanders, D. B., & Mirabel, I. F. 1996, ARA&A, 34, 749, doi: 10.1146/annurev.astro.34.1.749
Sanders, D. B., Soifer, B. T., Elias, J. H., Neugebauer, G., & Matthews, K. 1988, ApJL, 328, L35, doi: 10.1086/185155
Santarelli, A. D., Farag, E., Bellinger, E. P., et al. 2026, ApJL, 998, L4, doi: 10.3847/2041-8213/ae3713
Selina, R. J., Murphy, E. J., McKinnon, M., et al. 2018, ASP Conference Series, 517, 15. https://arxiv.org/abs/1810.08197
Shangguan, J., Chen, C.-H., Ho, L. C., et al. 2026, arXiv e-prints, arXiv:2606.04712, doi: 10.48550/arXiv.2606.04712
Shen, Y., & Liu, X. 2012, ApJ, 753, 125, doi: 10.1088/0004-637X/753/2/125
Shimwell, T. W., Hardcastle, M. J., Tasse, C., et al. 2026, A&A, 707, A198, doi: 10.1051/0004-6361/202557749
Smolčić, V., Novak, M., Bondi, M., et al. 2017, Astronomy & Astrophysics, 602, A1, doi: 10.1051/0004-6361/201628704
Wells, D. C., Greisen, E. W., & Harten, R. H. 1981, Astronomy and Astrophysics Supplement Series, 44, 363
Wilson, T. L., Rohlfs, K., & Hüttemeister, S. 2022, Tools of Radio Astronomy, 7th edn. (Cham: Springer), doi: 10.1007/978-3-031-28069-2
Wright, E. L. 2006, PASP, 118, 1711, doi: 10.1086/510102